Steady-State Distributions of O_2 and OH in the High Atmosphere and Implications in the Ozone Chemistry

A. J. C. Varandas†

Departamento de Química, Universidade de Coimbra, 3004-535 Coimbra, Portugal

Received: November 25, 2002

Although steady-state distributions are commonly accepted to be of the Boltzmann-type, such an assumption can be rather unrealistic when modeling the high atmosphere. Corroborating evidence is reported for the vibrational and rotational distributions of O_2 and OH from detailed trajectory calculations, which shows that the thermalization assumption is untenable at such environmental conditions. The implications in the O_x and HO_x catalytic cycles are also assessed.

1. Introduction

Ozone is known to be produced via photodissociation of O_2 by solar ultraviolet radiation followed by $O + O_2 + M$ recombination in excess O_2 ($M = N_2$ and O_2), while its destruction involves catalytic cycles of the form[1]

$$X + O_3 \rightarrow XO + O_2 \tag{1}$$

$$O_3 + h\nu \rightarrow O_2 + O \tag{2}$$

$$XO + O \rightarrow X + O_2 \tag{3}$$

$$\text{net: } 2O_3 + h\nu \rightarrow 3O_2 \tag{4}$$

where X = H, OH, HO_2, NO, halogen atoms, etc.; h is Planck's constant, and ν the photon frequency. Because they have the potential to change the biological makeup and possibly the climate of earth, enormous attention has focused to such catalytic sinks. However, only a relatively minor effort has been devoted[2,3−5] to find new ozone sources. This effort concentrated mostly on the role of electronic[2,3] and vibrational[2,4−6] excited states of O_2, with the role of the vibrational excitation of XO in eq 1 remaining unappreciated until recently.[5] It is on the energy distributions and role in the ozone chemistry of such vibrationally excited species that we focus in the present work.

Ozone photodissociation occurs via two electronic pathways: the singlet channel contributes about 90% to give $O(^1D) + O_2(a\ ^1\Delta_g)$ while the triplet channel contributes the remaining 10% to yield $O(^3P) + O_2(X\ ^3\Sigma_g^-)$. This leads to vibrationally excited O_2 in its ground electronic state [heretofore denoted as $O_2(v)$], which may react with any $XO(v)$ produced in reaction 1 to regenerate ozone. At wavelengths of 226, 230, 233, 234, and 240 nm, virtually all oxygen molecules formed from the O_3 photodissociation are vibrationally excited.[7] Typically, the $O_2(v)$ formed at 226 nm shows a bimodal vibrational distribution peaking in the vicinity of $v = 15$ and $v = 27$,[4] while at longer wavelengths the peak at $v = 27$ disappears,[7] although there is still an appreciable fraction of highly vibrationally excited O_2. Note that in the past it was the reaction

$$O(^1D) + O_3 \rightarrow 2O_2(v) \tag{5}$$

that was considered to be primarily responsible for $O_2(v)$ formation after photolysis of O_3 (rather than from direct photolysis[8]). In fact, reaction 5 may also yield appreciable amounts of vibrationally excited O_2 as it is sufficiently exoergic to excite simultaneously both molecules to $v = 20$. Moreover, because the yield of $O(^1D)$ is about 9 times larger than that of $O_2(v)$ in the initial ozone photodissociation process, only 10% or so of $O(^1D)$ needs to react in order to produce vibrationally excited O_2 in an amount comparable to that produced directly from the O_3 photodissociation. As additional sources of $O_2(v)$, we may mention the $O + O_3$ and $O + HO_2$ reactions: the former populates vibrational levels up to $v = 14$,[9] or even much higher,[10,11] and the latter up to $v = 13$.[6]

Although the quenching of $O_2(v)$ may not be rapid[3,12] (for a recent paper that addresses the earlier work, see ref 13), the suggestion has been made by Hickson et al.[12] that "...from the standpoint of atmospheric chemistry relaxation from high vibrational states of O_2 by the major atmospheric constituents, N_2 and O_2, is much too rapid for the photodissociation of these molecules to contribute significantly for the formation of ozone in the upper atmosphere".[12] However, for the temperatures and pressures of relevance at altitudes between 40 and 85 km (these cover the ranges[14] $160 \leq T/\text{K} \leq 280$ and $0.003 \leq P/\text{Torr} \leq 20$), the assumption of local thermodynamic equilibrium (LTE) may represent a massive simplification[4,5,10] while questioning such a remark.

A well-established example of a serious departure from LTE[15] is the observation of intense emission from highly vibrational ($v \leq 6$) and rotational ($N \leq 33$) excited states of OH in the mesosphere.[16] Among the first recognitions of vibrational *local thermodynamic disequilibrium* (LTD) effects is that of Meinel,[17] who correctly assigned the near-infrared night-time air-glow in the mesopause (85 km) to vibrationally excited hydroxyl radicals arising from the reaction[18−21]

$$H + O_3 \rightarrow OH(X\ ^2\Pi, v) + O_2 \tag{6}$$

Additional evidence comes from the vibrational quenching rate constants of $OH(v)$, which have been found to be considerably smaller than the reactive ones in collisions with O_3[22] and $O_2(v)$.[23]

† E-mail: varandas@qtvs1.qui.uc.pt.

10.1021/jp022483u CCC: $25.00
Published on Web 04/11/2003

Thus, both $O_2(v)$ and $OH(v)$ may exist in sufficient abundance to question the LTE assumption in atmospheric modeling simulations.

Of central importance in atmospheric modeling is therefore the choice of three possible vibrational distributions that can be formulated. If thermal equilibration exists, one has the popular Boltzmann distribution at a particular temperature. On the other hand, one has the nascent distributions of the relevant chemical species, namely, $O_2(v)$ from O_3 photolysis and $OH(v)$ from reaction 6. These distributions are fairly well understood at present but they can be modified in collisions with other environmental species (O_2 and N_2, which are by far the major constituents of the atmosphere). Thus, we are led to a third distribution which is actually the one present in the environment at discussion: *steady-state distribution*. This cannot be anticipated prior to considering the environment in its full photochemical complexity, although we may think that any modifications would be restored by subsequent photochemical and/or reactive processes. In this work, we attempt an answer to the question: what happens to the nascent distributions of vibrationally excited O_2 (formed from the ozone photolysis) and vibrationally excited OH (coming out of reaction 6) upon collisions with cold molecules in the high atmosphere? In so doing we assume that collisions with cold O_2 play the major role: collisions with N_2 and other minor atmospheric constituents are considered not to drastically alter the final results and are hence ignored.

The paper is organized as follows. Section 2 summarizes the dynamics calculations on the vibrational relaxation processes leading to the steady-state distributions. The possible implications of such results on the concentrations of O_3 and OH in the stratosphere and lower mesosphere are examined in section 3. In addition to some potentially important HO_x mechanisms (section 3.1) and dynamics calculations on an elementary reaction not studied thus far (section 3.1.1), this section contains the kinetics results obtained from a stationary-state analysis (section 3.2). The conclusions are in section 4.

2. Trajectory Simulation of Steady-State Distributions

All calculations reported in this work (see also section 3.1.1) employed the classical trajectory method as implemented in an extensively adapted version of the MERCURY/VENUS96[24] computer codes. Since the technical details concerning the integration of the classical equations of motion and boxing procedure for the assignment of vibrational and rotational quantum numbers are similar to those employed in previous work (refs 11 and 23, and references therein), no details will be given here.

2.1. The $O_2(v, j)$ Distributions. To study the involved $O_2(v') + O_2(v''=0)$ inelastic processes, we have employed the O_4 DMBE I[9] potential energy surface. The initial states of the colliding species were defined as follows. The initial vibrational distribution of the vibrationally hot oxygen has been chosen so as to mimic the distribution obtained from the O_3 photodissociation experiments[4] at 226 nm, while that of $O_2(v''=0)$ (cold oxygen) was assumed to be thermalized at $T = 255$ K. For the former, the relative micropopulation has been modeled by the following bimodal distribution:

$$P^{\text{hot}}(v') = \{\sum_k^2 a_k \exp[b_k(v' - c_k)^2]\}\mathscr{D}(v') \qquad (7)$$

where $\mathscr{D}(v') = {}^1/_2\{1 - \tanh[d(v' - e)]\}$ is a damping function which controls the antithreshold behavior for formation of vibrational excited products; $a_1 = 1.0052$, $a_2 = 0.9560$, $b_1 = 0.02242$, $b_2 = 0.076634$, $c_1 = 13.6570$, $c_2 = 28.7014$, $d = 2.39483$, and $e = 27.4546$ are the optimum least-squares parameters. At $T = 255$ K, a thermalized vibrational distribution leads essentially to a single peak at $v'' = 0$, and hence all calculations have been done by considering the cold O_2 molecules in their ground vibrational state. A thermalized ($T = 255$ K) rotational distribution has also been assumed for the vibrationally cold O_2 molecules. However, the nascent rotational distribution of the vibrationally excited oxygen molecules resulting from the ozone photodissociation will certainly differ from a thermalized one. Unfortunately, such a distribution is unknown at present, and hence we have assumed that it could be represented by the rotational distribution observed by Daniels and Wiesenfeld[8] for the product $O_2(v=12)$ molecules in their ozone photolysis experiments at 248 nm. From an analysis of their results, we have concluded that their rotational distribution is well reproduced by summing a Boltzmann distribution for $T = 600$ K to the nascent distribution indicated in Figure 12 of their paper (this carries a weighting factor of 355 when the maxima of the two separate distributions are both set to unity). Thus, we have replaced the former by a Boltzmann rotational distribution for $T = 255$ K while leaving the second distribution and corresponding weighting factor untouched.

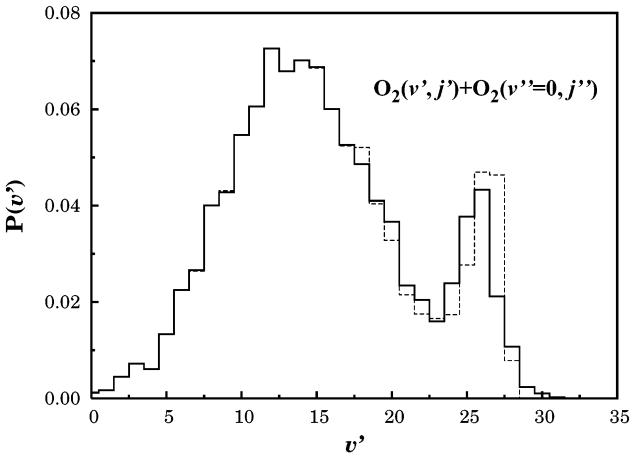

Figure 1. A comparison of the initial and final vibrational distributions for the vibrationally excited oxygen in the simulation study of the $O_2(v') + O_2(v''=0)$ inelastic collisional process carried out in the present work. The results refer to a total of 25000 trajectories, being the initial and final vibrational distributions shown by the dashed and solid lines, respectively. The translational energy is thermalized at $T = 255$ K.

Except for the trivial vibrational distributions of the cold oxygen molecules (where only the $v = 0$ state is basically populated for $T = 255$ K), the initial vibrational and rotational distributions employed for the simulations of the present work are displayed in Figures 1 and 2. In fact, a computer simulation employing the traditional approach (ref 25, and references therein) has shown that such distributions can be accurately mimicked with a few thousand trajectories, and it is the very conservative results obtained in this way by using a total of 25000 trajectories that we consider as the initial distributions. Also shown in Figures 1 and 2 are the final distributions obtained after the collisional simulation study. Despite some significant energy transfer, the results indicate that both the vibrational and rotational final energy distributions maintain most of the features of the corresponding initial (nascent) distributions.

Of particular relevance for the ozone chemistry are the differences between the initial and final vibrational distributions

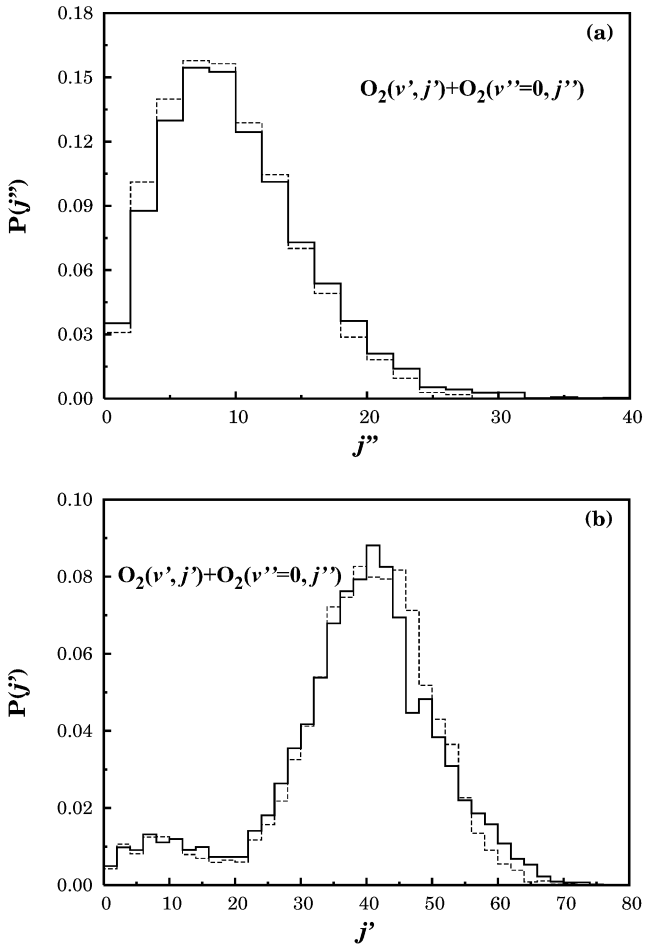

Figure 2. As in Figure 1 but for the rotational distributions of in the $O_2(v') + O_2(v''=0)$ inelastic collisional process: (a) $O_2(v''=0)$ and (b) $O_2(v')$.

of the vibrationally hot oxygen molecules (as usual, the indices "i" and "f" will be used to label the initial and final states). Clearly, the most significant changes refer to the vibrationally excited states $v' \geq 20$, where the major alterations correspond to an increase of the populations for $v'_f = 25$ and $v_f' \geq 28$ at the expense of $v'_f = 27$. For small values of v' (for example, $v' \leq 15$ or so), the differences between the two distributions are negligible, which may be explained from the larger size of the vibrational quanta at low v' and the small translational energies involved. Leaving aside the translational energy, it is plausible to expect rotational-to-rotational (R−R) and rotational-to-vibrational (R−V) energy transfer (the latter involving primarily high v' states) to be the most efficient mechanisms since a smaller amount of energy is transferred. As a result, the second peak in the final distribution of the vibrationally hot O_2 molecules arises at $v'_f = 26$, rather than at its original value of $v'_i = 27$. We emphasize that the molecules are left after the collisional process sufficiently energetic to react with vibrationally excited hydroxyl radicals leading to ozone formation.[23,26] Note also that the population of $v'_f = 29$ has increased slightly, while the states $v'_f = 30$ and $v'_f = 31$ have also become populated. Although such excitations occurred only to a small extent, it is also true that they have led to $O_2(v)$ species with a higher propensity for reaction. A final remark to note: if one had instead assumed as the initial rotational distributions those obtained from a quasiclassical trajectory study[11] for the reaction $O + O_3 \rightarrow O_2(v) + O_2$, then some vibrational warming of the final vibrational distributions with respect to the initial ones could even be observed at the expenses of a somewhat more pronounced V−R energy transfer; note that the $O_2(v)$ molecules are formed in this reaction highly rotationally excited.

Similarly, no drastic changes are visible in the rotational distributions. Specifically, one observes some rotational warming for the vibrationally cold O_2 molecules, while the bimodal rotational distribution of the vibrationally hot O_2 molecules shows on average hardly any changes, except for a small shift to the left of the second peak corresponding to the O_2 rotational distribution from the photodissociated ozone.

Despite the fact that the initial and final distributions show similar patterns, this by no means implies that there has not been a significant energy transfer at the microscopic level. In fact, although only six (<0.1%) out of the total number of trajectories ran led to a vibrational excitation of the cold O_2 molecules to $v''_f = 1$, there have been 3529 (14%) vibrationally hot molecules that experienced vibrational relaxation. However, if rotational transitions are considered, then the number of vibrationally cold O_2 molecules that suffered a rotational transition raises to 7306 (29%), while this number increases further to 16548 (66%) for the hot ones. Table 1 summarizes in more detail the important energy transfer processes involved. For simplicity, they have been catalogued according to their V−V and V−R characteristics, leaving aside the translational degrees of freedom. For example, a process labeled V−R may also have a strong component of vibrational-to-translation energy transfer, which we have made no attempt to discriminate in this work. Note that the four vibrationally cold O_2 molecules which transited to $v''_f = 1$ involved a $(v',0) \rightarrow (v'-1,1)$ transition, while the $(v',0) \rightarrow (v'-1,0)$ transitions amounted to 2333. From these results, one may calculate the thermal rate coefficients as

$$k^x(T) = g_e(T)\left(\frac{8k_BT}{\pi\mu}\right)^{1/2}\sigma^x(T) \qquad (8)$$

where x specifies the event under consideration, $g_e = {}^1/_3$ is the electronic degeneracy factor (apparently considered to be unity in ref 13), k_B is the Boltzmann constant, μ is the reduced mass of the colliding diatomic molecules, and T is the temperature in Kelvin. In turn, σ^x is the calculated cross section $\sigma^x = \pi b_{max}^2 N^x/N$, with $b_{max} = 16.3a_0$ being the maximum impact parameter. The calculated thermal rate coefficients are also shown in Table 1. Of these, the result for the total V−V energy transfer may be compared with the corresponding value obtained from Table 3 of ref 13 at $T = 300$ K using a potential energy surface which does not allow for reaction. One obtains for the latter (suitably multiplied by g_e) the value of $\sum_{v'} k_{v',0\rightarrow v'-1,1} = 2.5 \times 10^{-13}$ cm^3 s^{-1}, which compares well with the result of $(1.1 \pm 0.4) \times 10^{-13}$ cm^3 s^{-1} reported in Table 1 for $T = 255$ K. Finally, we observe from Table 1 that multiquanta vibrational transitions tend to predominate, possibly involving high v'_i states since most vibrational transitions occurred for such a regime. This result may be explained from the smaller size of the associated vibrational quanta, allowing a wider variety of combinations susceptible of matching the vibrational and rotational energy spacings of the cold O_2 molecules.

2.2. The OH(v, j) Distributions. Despite the fact that a detailed dynamics study of the $OH(v') + O_2(v''=0)$ vibrational relaxation process has been reported,[26] the major role played by such a process in the title issue warrants a simulation similar to that presented in the previous paragraph but for the nascent versus steady-state distribution of $OH(v')$. We emphasize that only collisions of $OH(v')$ with vibrationally cold O_2 are considered, leaving aside the reactive processes which have also been a subject of previous studies.[23,27,28] For consistency, all

TABLE 1: A Summary of Some Energy Transfer Processes Involved in the $O_2(v',j') + O_2(v''=0,j'')$ Inelastic Collisional Simulation Study at $T = 225$ K Carried out in the Present Work[a]

type	process[b] (=x)	N^x [c]	probability (%)	$k^x_{v'_i j'_i v''_i j''_i \rightarrow v'_f j'_f v''_f j''_f}$ ($10^{-13} \times$ cm^{3}s^{-1})
V−V	$O_2(v'_i,j'_i) + O_2(v''_i=0,j''_i) \rightarrow O_2(v'_f=v'_i-1,j'_f) + O_2(v''_f=1,j''_f)$	6	<0.1	1.1 ± 0.4
V−R	$O_2(v'_i,j'_i) + O_2(v''_i=0,j''_i) \rightarrow O_2(v'_f=v'_i-1,j'_f) + O_2(v''_f=0,j''_f)$	2333	9.3	420 ± 8
V−R	$O_2(v'_i,j'_i) + O_2(v''_i=0,j''_i) \rightarrow O_2(v'_f=v'_i-2,j'_f) + O_2(v''_f=0,j''_f)$	97	0.4	17 ± 2
V−R	$O_2(v'_i,j'_i) + O_2(v''_i=0,j''_i) \rightarrow O_2(v'_f=v'_i-n,j'_f)$[d] $+ O_2(v''_f=0,j''_f)$	1093	4.4	197 ± 6
V−R	$O_2(v'_i,j'_i) + O_2(v''_i=0,j''_i) \rightarrow O_2(v'_f \neq v'_i,j'_f) + O_2(v''_f=0,j''_f)$	3529	14.1	635 ± 8
R−R	$O_2(v'_i,j'_i) + O_2(v''_i=0,j''_i) \rightarrow O_2(v'_f=v'_i,j'_f) + O_2(v''_f=0,j''_f)$	4372	17.5	787 ± 11

[a] The maximum impact parameter in this simulation has been $b_{max} = 16.3a_0$. [b] If a quantum level is left unspecified, the reported quantity refers to all possible initial states. [c] N^x represents the number of effective events out of a total number of $N = 25000$ trajectories ran. [d] $n \geq 3$.

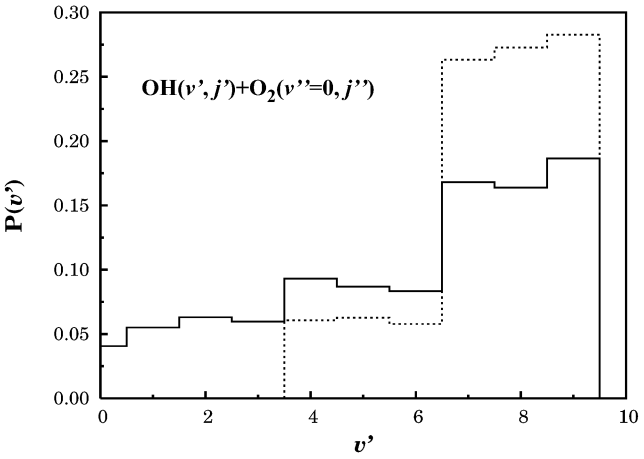

Figure 3. A comparison of the initial and final vibrational distributions for the vibrationally excited hydroxyl radical in the simulation study of the $O_2(v') + O_2(v''=0)$ inelastic collisional process carried out in the present work. The results refer to a total of 20000 trajectories, being the initial and final vibrational distributions shown by the dashed and solid lines, respectively.

calculations employed the HO_3 DMBE I potential energy surface.[29] As in the case of $O_2(v') + O_2(v''=0)$, the vibrationally cold O_2 molecules at $T = 255$ K are considered to be in their ground vibrational state, while the OH(v') nascent vibrational distribution has been taken from Ohoyama et al.;[18] see Figure 3. In turn, the relevant rotational populations[30] used in the present simulation are those of Cosby[30] for the six OH Meinel bands (4−0, 5−1, 6−1, 7−2, 8−3, 9−4) in the coadded data set "order". These bands were recorded simultaneously by the HIRES schelle spectrograph on the Keck I telescope during the 14 months in the period Dec 1994−May 1997; a description of this data set can be found in ref 31. Such populations refer to the upper state rotational levels and were conveyed to us as the natural logarithm of the ratio of the population divided by the rotational degeneracy, namely, $\ln[N(J')/(2J'+1)]$, where J' is the total rotational quantum number. Assuming the Hund's case (b) limit, the nuclear rotation quantum number N' for the spin−orbit levels F_1 is given by $N' = J' + {}^1/_2$; for F_2, $N' = J' - {}^1/_2$. We have used N' (denoted j' heretofore for consistency), although we should note that for OH each N' will consist of two levels separated by significant energies at low N' (actually there are four levels if we also consider the nondegeneracy of the lambda doublets, but this *e*/*f* splitting is significant only at high J', e.g., it is[30] 5 cm^{-1} at $J = 17.5$ in F_1).

Despite the care taken in deriving the OH(v') rotational populations, the authors[30] cannot warrant that there are no systematic changes in the absolute populations from band to band. Hence, the relative vibrational populations may not be quantitative. Moreover, they represent season-averaged values for OH in the nightglow (i.e., created by the H + O_3 reaction) subject to collisional relaxation before emitting.[30] Such a relaxation is most likely responsible[30] for the two-temperature rotational distributions observed in the night-glow data: a low temperature (∼200 K) in the rapidly relaxed lower rotational levels ($j' < 5$) and a much higher apparent temperature in the slowly relaxed higher rotational levels (for a two-temperature rotational distribution observed in calculations for the O + O_3 reaction, see ref 11). Note that Polanyi et al.[32,33] have also carried out an experiment where they measured the Meinel emission of nascent OH created by crossed beams of H and O_3. A comparison between the nightglow (partially relaxed) values of Osterbrock et al.[31,30] and Polanyi's[32,33] nascent (but also partially relaxed) values show significantly lower rotational populations with increasing rotational excitation. Of course, such differences may have implications on the result of the current simulation, although no attempt will be made here to quantitatively assess their magnitude. Llewellyn and Long[34] derived nascent rotational temperatures for $v = 7-9$ from Polanyi's[32,33] data. These are found to be somewhat smaller than Cosby's[30] temperatures for $v = 7$ but larger for $v = 8$ and $v = 9$. It should further be noted that the nascent OH rotational and vibrational distributions are dependent on the reaction producing the OH; see ref 35 for an example of OH produced from H_2O_2.

Figure 4a shows the effective nascent rotational distribution of OH employed in the simulations of the present work. It represents the result obtained from the rotational sampling done according to Cosby's[30] relative rotational micropopulations for the six OH Meinel bands. In turn, Figure 4b depicts the corresponding rotational distribution for the vibrationally cold O_2 molecules, which was taken as the Boltzmann distribution for $T = 255$ K. Although such rotational distributions are well mimicked with a few thousand trajectories, a very conservative number of 20000 trajectories has been employed in the present simulation. Also shown for comparison in Figures 3 and 4 are the final distributions obtained after the $OH(v'_i) + O_2(v''_i=0) \rightarrow OH(v'_f) + O_2(v''_f)$ vibrational−rotational relaxation. Clearly, there is significant energy transfer, with the results indicating that the final vibrational steady-state distribution maintains roughly 70% of the initial populations for the three highest vibrational levels ($v' = 7-9$). Although one might conjecture that this would inhibit the OH(v') reactivity in a corresponding proportion, the quantitative effect is likely to be significantly less than the observed 30% reduction for the $v' = 7-9$ populations since the lower OH vibrational states may also contribute to the reaction with $O_2(v'')$ to form ozone. In fact, the populations of the $v' = 4-6$ states is found to increase by 60% or more with respect to the initial values, with similar populations being observed for $v'_f \leq 3$ which were initially zero. It should also be pointed out that some fraction of the OH-(v'_f=9) molecules have an energy significantly higher that the quantum mechanical value associated to this state. Given the limitations of the boxing procedure, such an observation may

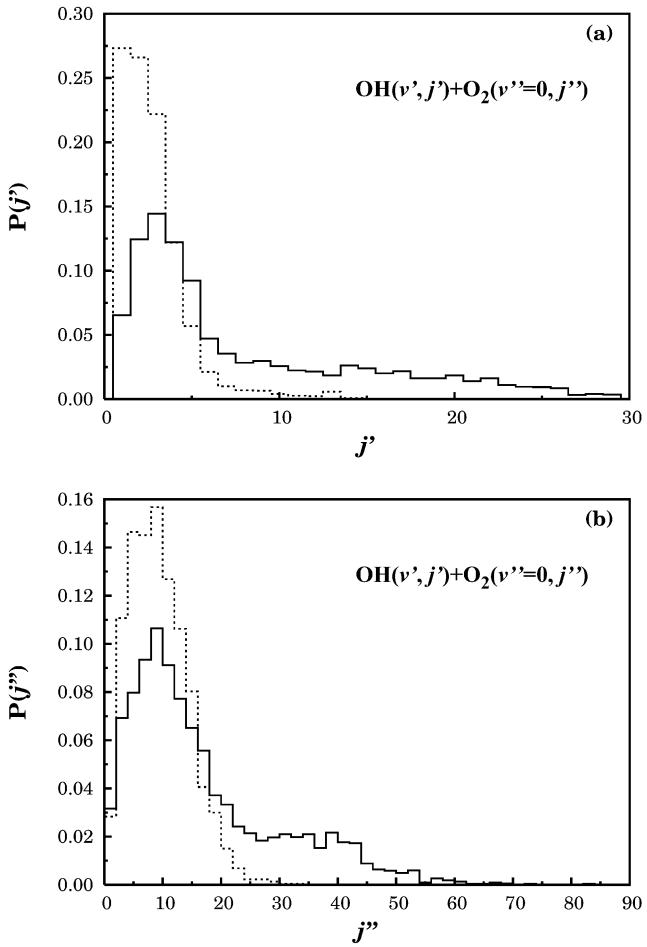

Figure 4. As in Figure 1 but for the rotational distributions of (a) OH(v') and (b) O_2(v'') in the OH(v') + O_2(v''=0) inelastic collisional process.

be taken as evidence to support the faint OH(v'=10) emission line recently detected in the night air-glow.[31] Needless to say, these "$v' = 10$ states" would contribute to enhance further the reactivity and, hence, support our estimate of a reduction <30% on the reactivity of OH(v') in collisions with O_2(v'') when one replaces the OH(v') nascent distribution by the steady-state one. In this regard, it is not excessive to emphasize that the initial rotational distributions employed for the simulations are partially relaxed, which gives further confidence to the expectation of a scaling down in reactivity significantly smaller than 30%.

Another interesting result concerns the rotational distributions. One observes that the depletion of the low j' states in the initial ("nascent") rotational distribution of OH(v') is compensated by a rotational warming of the final (steady-state) one. From energetic considerations, one expects that highly excited rotational states (populated up to $j'_f = 30$) correspond to low v'_f levels. This is an interesting result in itself, since there is strong evidence from the mesosphere that highly excited rotational levels as high as 30−33 are present,[16] although such levels were completely undetected from Polanyi's[32,33] pioneering studies. Highly rotationally excited states have also been recently observed for the OH(v'=0,1) products in the reaction of fast hydrogen atoms with ozone.[36] It is not clear though whether the high j populations are formed directly through the reaction 6 or through a secondary energy transfer process.[36] Since such highly rotationally excited products could not be observed from our H + O_3 dynamics studies,[37] we are tempted to believe that they may (at least partly) be an outcome of an unusually efficient V−R collisional energy transfer with the nascent OH(high v', low j') states. This is corroborated from the last entry in Table 2, which shows that pure R−R transitions are extremely unlikely.

As already noted, important energy transfer processes have occurred. For example, 7.3% of the vibrationally cold O_2 molecules transited to $v''_f = 1$, but of these, only 0.6% and 0.9% involved the processes (v',0) → ($v'-m$,1), with $m = 1-2$ in that order. Even smaller fractions of cold O_2 molecules transited to $v''_f = 2$ and $v''_f = 3$, respectively, 0.8% and 0.1%. The total deexcitation of OH(v') amounted to 41%. Table 2 summarizes some of the thermal rate coefficients obtained from eq 8 with $g_e(T) = {}^1/_3[1 + \exp(-205/T)]^{-1}$; all other symbols retain their meanings corresponding to those previously assigned. Thus, σ^x is the calculated cross section for process x, with the maximum impact parameter being now $b_{max} = 11.3a_0$. The only piece of experimental data that may be offered for comparison is the collisional removal rate constant reported by Chalamala and Copeland[38] for the OH($X^2\Pi$,v=9) radical in collisions with ground state O_2. They report a value of $(17 \pm 11) \times 10^{-12}$ cm^3 s^{-1} at room temperature. This is about 3 times smaller than the total deexcitation rate of $(62 \pm 1) \times 10^{-12}$ cm^3 s^{-1} extracted from the present calculations, which is in turn about twice smaller than our previously reported[26] estimate. Such a difference may be attributable to the fact that the rotational states of the colliding species have then[26] been fixed at $j'_i = j''_i = 1$. Thus, rotational excitation seems to play a significant role on the removal rate constants in OH(v') + O_2(v''=0) collisions, an issue that warrants further investigation. As in the case of O_2(v'_i,j'_i) + O_2(v''_i=0,j''_i) discussed above and in ref 26, multiquanta vibrational transitions are found to dominate.

3. Possible Effect on the Concentrations of O_3 and HO_2 in the Stratosphere and Lower Mesosphere

3.1. Some Potentially Important HO_x Mechanisms. We examine here some potentially important HO_x (denoted also HO_{y+3}) mechanisms which have not been investigated thus far. We start by recalling that the concentration of H atoms is rather small[39] for altitudes up to ~40 km. Thus, to a first approximation, the mechanism $y = 0$ may be ignored at such altitudes. Moving upward, [H] is known[39] to slightly exceed [OH] and [HO_2] above ~60 km. In turn, [O_3] shows[39] a decreasing pattern with altitude from its maximum at ~40 km, being always larger than [H], [OH], and [HO_2]. The study of the HO_{y+3} mechanisms may then be split into $y = 1$ and 2 for altitudes below ~40 km and into $y = 0-2$ for higher altitudes. Moreover, owing to the disparity of the rate constants for reaction 1 [for H + O_3, OH + O_3, and HO_2 + O_3 at 255 K, one has[40] 2.1×10^{-11}, 3.8×10^{-14} (this can be much larger if OH is vibrationally excited[22]), and 1.3×10^{-15} cm^3 s^{-1}], a further split of the latter into $y = 0$ and 1 and into $y = 2$ is plausible.

The $y = 1$ and 2 mechanism assumes the form

$$3[OH + O_3 \rightarrow HO_2(v) + O_2] \quad (9)$$

$$HO_2 + O_3 \rightarrow OH + O_2(v') + O_2 \quad (10)$$

$$4[O_3 + h\nu \rightarrow O_2(v'') + O(^3P)] \quad (11)$$

$$HO_2(\mathbf{v}) + O_2(v'') \rightarrow O_3 + OH \quad (12)$$

$$HO_2(\mathbf{v}) + O_2(v'') \rightarrow OH + O_2 + O(^3P) \quad (13)$$

$$HO_2(\mathbf{v}) + O_2(v'') \rightarrow HO_2 + 2O(^3P) \quad (14)$$

TABLE 2: A Summary of Some Energy Transfer Processes Involved the (v',j') + (v''=0,j'') Inelastic Collisional Simulation Study at T = 255 K Carried out in the Present Work[a]

type	process[b] (=x)	N^x [c]	probability (%)	$k^x_{v'_i j'_i, v''_i j''_i \rightarrow v'_f j'_f, v''_f j''_f}$ ($10^{-13} \times$ cm^{3}s^{-1})
V−V	$OH(v'_i,j'_i) + O_2(v''_i=0,j''_i) \rightarrow OH(v'_f=v'_i-1,j'_f) + O_2(v''_f=1,j''_f)$	123	0.6	11 ± 1
V−R	$OH(v'_i,j'_i) + O_2(v''_i=0,j''_i) \rightarrow OH(v'_f=v'_i-1,j'_f) + O_2(v''_f=0,j''_f)$	1131	5.7	103 ± 3
V−R	$OH(v'_i,j'_i) + O_2(v''_i=0,j''_i) \rightarrow OH(v'_f=v'_i-2,j'_f) + O_2(v''_f=0,j''_f)$	1090	5.4	99 ± 3
V−R	$OH(v'_i,j'_i) + O_2(v''_i=0,j''_i) \rightarrow OH(v'_f=v'_i-m,j'_f)^d) + O_2(v''_f=0,j''_f)$	4418	22.1	401 ± 5
V−R	$OH(v'_i,j'_i) + O_2(v''_i=0,j''_i) \rightarrow OH(v'_f \neq v'_i,j'_f) + O_2(v''_f=0,j''_f)$	6639	33.2	603 ± 5
V−R	$OH(v'_i,j'_i) + O_2(v''_i=0,j''_i) \rightarrow OH(v'_f \neq v'_i,j'_f) + O_2(v''_f,j''_f)$	8266	41.3	750 ± 6
R−R	$OH(v'_i,j'_i) + O_2(v''_i=0,j''_i) \rightarrow O_2(v'_f=v'_i,j'_f) + O_2(v''_f=0,j''_f)$	n.o.[e]	n.o.	n.o.

[a] The maximum impact parameter in this simulation has been $b_{max} = 11.3a_0$. [b] If a quantum level is left unspecified, the reported quantity refers to all possible initial states. [c] N^x represents the number of effective events out of a total number of N = 20000 trajectories ran. [d] $m \geq 3$. [e] n.o. = not observed for the specified state conditions.

$$O_2(v') + O_2(v'') \rightarrow O_3 + O(^3P) \quad (15)$$

$$8[O(^3P) + O_2 + M \rightarrow O_3 + M] \quad (16)$$

$$\text{Net: } 3O_2 + 4h\nu \rightarrow 2O_3 \quad (17)$$

where **v** denotes collectively the three vibrational quantum numbers of the triatomic, and $O_2(v' \geq v'_0)$ [denoted simply by $O_2(v')$] is an oxygen molecule formed via chemical reaction, which is typically less vibrationally excited than the $O_2(v'' \geq v''_0)$ molecules formed by ozone photolysis. Thus, within the spirit of LTD, they will be treated as distinct species. Note that reactive collisions involving two $O_2(v'' \geq v''_0)$ molecules are ignored since such a second-order process in $O_2(v'')$ is less likely to happen, while pertaining more to O_x[5] rather than HO_x chemistry. If the reactions 9, 11, 12−14, and 16 are instead considered with appropriate stoichiometric factors, one obtains the $y = 1$ mechanism[5] whose net result is $OH + 2O_2 + 3h\nu \rightarrow O_3 + HO_2$. In turn, the $y = 0$ mechanism[5] involves the reactions $OH(v') + O_2(v'') \rightarrow O_3 + H$, $OH(v') + O_2(v'') \rightarrow O_2 + O + H$, and $OH(v') + O_2(v'') \rightarrow OH + 2O$, leading to the net result $H + 2O_2 + 3h\nu \rightarrow O_3 + OH$. For the $y = 0$ and 1 mechanism, one then obtains $H + 4O_2 + 6h\nu \rightarrow 2O_3 + HO_2$, showing that it is a source of O_3 and HO_2 at the expense of OH. This result may be of significance to explain the so-called "OH surplus" in the lower mesosphere.[41,42]

Alternatively, we may formulate the $y = 0$ and 1 mechanism in a way similar to $y = 1$ and 2 by replacing OH by H and HO_2 by OH. One then has

$$3[H + O_3 \rightarrow OH(v) + O_2] \quad (18)$$

$$OH + O_3 \rightarrow H + O_2(v') + O_2 \quad (19)$$

$$4[O_3 + h\nu \rightarrow O_2(v'') + O(^3P)] \quad (20)$$

$$OH(v') + O_2(v'') \rightarrow O_3 + H \quad (21)$$

$$OH(v') + O_2(v'') \rightarrow O_2 + O(^3P) + H \quad (22)$$

$$OH(v') + O_2(v'') \rightarrow OH + 2O(^3P) \quad (23)$$

$$O_2(v') + O_2(v'') \rightarrow O_3 + O(^3P) \quad (24)$$

$$8[O(^3P) + O_2 + M \rightarrow O_3 + M] \quad (25)$$

$$\text{Net: } 3O_2 + 4h\nu \rightarrow 2O_3 \quad (26)$$

The major difference with respect to the sum of $y = 0$ and $y = 1$ mechanisms[5] is therefore the assumption of reaction 19 instead of 9. In fact, a careful analysis of the output from recent trajectory calculations[22,43] has shown that the reaction 19 occurs when OH has one or more quanta of vibrational excitation (for ground vibrational OH, it is energetically allowed only for translational energies above ~7.5 kcal mol^{-1}). By considering eqs 9−17 and eqs 18−26, one obtains the $y = 0$−2 mechanism. We emphasize that the above mechanisms find support on theoretical studies of the involved elementary chemical reactions (ref 5, and references therein), including those for the reaction 14 which are reported next.

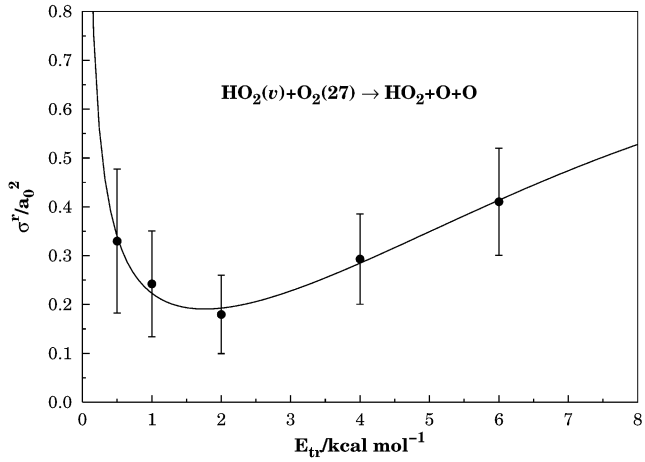

Figure 5. Calculated cross sections for the reaction $HO_2(v) + O_2(v''=27) \rightarrow HO_2 + 2O$. Indicated by the dots (with corresponding 68% error bars) are the actual calculations, while the line indicates the fit to eq 27.

*3.1.1. The Reaction HO_2(**v**) + $O_2(v'') \rightarrow HO_2 + 2O$.* Although no evidence has been reported thus far for this reaction, trajectory calculations have shown that it occurs when the vibrational excitation in HO_2 exceeds 36 kcal mol^{-1} (this is the average vibrational energy of the HO_2 products in the $OH(v=0) + O_3$ reaction, which is the main source of hydroperoxyl radicals in the middle atmosphere). In fact, rotationally thermalized calculations for the reaction HO_2(**v**) + $O_2(v''=27) \rightarrow HO_2 + 2O$ with such a vibrational excitation democratically distributed by the three vibrational normal modes of HO_2 gives a rate constant of $k = (4.6 \pm 0.8) \times 10^{-13}$ cm^3 s^{-1} at T = 255 K (a total of 12500 trajectories have been run, with an optimized maximum impact parameter of $b_{max} = 5.9a_0$). A somewhat smaller value is obtained when O_2 is fixed at the rotational state $j = 1$, while HO_2 is kept thermalized. Figure 5 shows that the calculated cross sections given in Table 3 are then well fitted by the excitation function

$$\sigma^r = CE_{tr}^{-n} + BE_{tr}^2 \exp(-mE_{tr}) \quad (27)$$

with $B = 0.0228$, $C = 0.2032$, $m = 0.1382$, and $n = 0.7157$ being the optimum least-squares parameters; units are such that

TABLE 3: Summary of the Calculations for the Reaction[a] $HO_2(v) + O_2(v''=27) \rightarrow HO_2 + 2O$

E_{tr} (kcal mol^{-1})	$b_{max}(a_0)$	$\sigma^r \pm \Delta\sigma^r(a_0^2)$
0.5	7.9	0.33 ± 0.15
1.0	6.8	0.24 ± 0.11
2.0	5.9	0.18 ± 0.08
4.0	5.3	0.29 ± 0.09
6.0	5.3	0.41 ± 0.11

[a] See the text.

with the translational energy E_{tr} in kcal mol^{-1} the cross section is in a_0^2. From eq 27, the corresponding specific rate constant can be calculated analytically[43] as a function of temperature yielding $k = 1.7 \times 10^{-13}$ cm^3 s^{-1} at $T = 255$ K. This is roughly one-half of the rotationally thermalized value reported above, although the 68% error bars in the reactive cross sections are appreciable despite the fact that 3000 trajectories have been run per translational energy. Thus, conversely to findings in studies of other reactions,[6,44,45] rotational excitation seems to play an important role as it promotes the dissociation of vibrationally hot O_2 by increasing its energetic content. However, the salient feature is the magnitude of the total reactive rate constant which is found to be 2 orders of magnitude larger than for $HO_2 + O_3$; a detailed study of such a reaction will appear elsewhere.[46]

3.2. Kinetics Results. The possible effect of the $y = 1$ and 2 mechanism on the concentration of stratospheric O_3 is investigated by using the stationary-state assumption for $[O_2(v')]$ and $[HO_2(v)] + [O_2(v'')]$. This may be rationalized from the magnitude of the rate constants of reactions 9 and 10, which suggest that $O_2(v')$ may be best treated independently from the other two intermediate species. Substitution of such stationary-state concentrations into the rate of additional O_3 production due to reactions 12−15 gives

$$\frac{d[O_3]}{dt} = \frac{k}{2k_D}\left(4\int_{\lambda<\lambda_0} J_{O_3}(\lambda, z,\chi)\Phi_{v''\geq v''_0}(\lambda)d\lambda + 3k_9[OH] - k_{10}[HO_2]\right)[O_3] + \frac{2k_{10}k_{15}}{k'_D}[HO_2][O_3] \quad (28)$$

where $J_{O_3}(\lambda, z,\chi)$ is the photodissociation coefficient of O_3 which depends on the wavelength λ, altitude z, and zenith angle χ; $\Phi_{v''\geq v''_0}(\lambda)$ is the quantum yield for production of $O_2(v''\geq v''_0)$, and k_n is the rate constant for reaction n. In turn, k_D and k'_D are the total collisional removal rates of $HO_2(v)$ and $O_2(v'')$, respectively, which may be approximated by $k_D \sim k_{12} + k_{13} + k_{14}$ and $k'_D \sim k_{15}$. Moreover, $k = k_{12} + k_{13} + 2k_{14}$, with the factor 2 accounting for the fact that O recombines fast with O_2 to form O_3.

Relative to the rate of O_3 production in the conventional mechanism, the fractional additional odd oxygen production assumes the form

$$F_{12} = \left\{\frac{k}{2k_D}(4R_{v''\geq v''_0}R_{\lambda_0}J_{O_3\rightarrow O(^3P)} + 3k_9[OH]) + \left(\frac{2k_{15}}{k'_D} - \frac{k}{2k_D}\right)k_{10}[HO_2]\right\}\frac{[O_3]}{8J_{O_2}[O_2]} \quad (29)$$

where the constant yield $\Phi_{v''\geq v''0}(\lambda) = \Phi R_{v''\geq v''0}$ [Φ is the quantum yield of reaction $O_3 + h\nu \rightarrow O_2 + O(^3P)$ for production of O_2 in a state $v'' \geq v''_0$, and $R_{v''\geq v''0}$ is the probability for such a reaction to produce such high vibrational states] has been assumed,[4] $R_{\lambda 0} = J_{O_3}(\lambda,z,\chi)d\lambda/\int J_{O_3}(\lambda,z,\chi)d\lambda$ is the fraction of O_3 photolysis which takes place at wavelengths shorther than λ_0, and $J_{O_3\rightarrow O(^3P)} = \Phi J_{O_3}(\lambda,z,\chi)d\lambda$ is the total O_3 photolysis rate constant leading to $O(^3P)$. Note that the wavelength-integrated photolysis rate of O_2 is $2J_{O_2}[O_2]$, and hence the extra factor of 4 accounts for the fact that there are four photons consumed in the mechanisms 9−16. For simplicity, we consider now the O_3 photolysis to be at $\lambda = 226$ nm, $v''_0 = 26$, $R_{v''\geq 26} = 0.081$, and the long wavelength threshold for production of vibrational excited O_2 to be $\lambda_0 = 243$ nm, since these data can be taken directly from ref 4. We should point out that such conditions may be somewhat too restrictive as the calculations[23,28] have shown that $(v',v'') = (3,12)$ is about the lowest vibrational combination in $OH(v') + O_2(v'')$ collisions capable of leading to reaction. Table 4 gives the ratios F_{12} so obtained (we have further assumed $k = k_D$ and $k'_D = k_{15}$). As seen, the proposed new source produces O_3 at rates which range from 0.15 to 0.04 the principle O_2 photodissociation source as the altitude varies from 40 to 55 km. Note that the second term in eq 29 gives a minor contribution due to the smaller magnitude of k_D relative to k_{10}.

In turn, the ratios F_{01} can be approximated by

$$F_{01} \simeq (2R_{v''\geq v''0}R_{\lambda_0}J_{O_3\rightarrow O(^3P)} + {}^3/_2k_h[H])\frac{[O_3]}{8J_{O_2}[O_2]} \quad (30)$$

where k_h is the rate of the $H + O_3$ reaction; since the rate constant for the reaction $OH + O_3 \rightarrow H + O_2(v') + O_2$ is expected to be rather small at typical stratospheric temperatures even for OH radicals with one quantum of vibrational excitation, the corresponding contribution can be neglected. Table 4 shows that F_{01} dominates at high altitudes due to the increasing role of atomic hydrogen. In fact, although F_{01} assumes values 3 times smaller than those obtained from the Wodtke[4] mechanism at 40 km (0.48[4]), it becomes 30 times larger than that at 55 km. This estimate is smaller than for $y = 0$[5] and about twice larger than for $y = 0-2$, which may be explained by the lower efficiency of the photons used to sustain less reactive processes. Yet, even in this less favorable situation, the ratio of additional odd oxygen production is more than 1 order of magnitude larger than predicted by the Wodtke mechanism at 55 km!

In an attempt to find a more realistic answer, consider what happens to a newly formed $OH(v')$ species. Two basic situations can arise. The first is a collision of $OH(v')$ with a N_2 molecule. Since N_2 occupies 80% of the atmosphere, the question is then to know whether such a collision can still leave OH sufficiently hot to react with $O_2(v'')$. Measurements have shown[38] that N_2 is a slow collider leading to a slow decrease in the population of $OH(v=9)$, while O_2 is the dominant quencher. The remaining 20% probability refers to a collision of the nascent $OH(v')$ with molecular oxygen. Using the calculated steady-state distributions, the chance of such a collision to involve an $O_2(v''\geq 24)$ is estimated to be about 12%, becoming 8% if one takes instead $O_2(v''\geq 25)$. By considering now that the probability of obtaining $OH(v'\geq 3)$ is about 80%, one obtains for the composite probability of a reactive collision a value of 8%. One might argue that a further reduction by a power of 10 should be introduced to account for the proportion of $O_2(v'')$ directly formed in the ozone photodissociation. However, such a reduction might lead to a severe and most likely erroneous underestimation of the $O_2(v'')$ concentration having in mind eq 5, and hence, it has not been considered. Of special significance though is the fact that vibrational deactivation in $OH(v') + O_2(v'')$ collisions (which is dominated by multiquanta vibrational transitions) has been found[23] to be insufficient for quenching the population of

TABLE 4: Ratios of Additional Ozone Production[a] Obtained from Mechanisms $y = (0,1)$ and $y = (1,2)$'

altitude (km)	$10^4 J_{O_3 \rightarrow O(^3P)}$ (s^{-1})	$10^{-10}[O_3]$ (cm^{-3})	$10^{10} J_{O_2}$ (s^{-1})	$10^{-15}[O_2]$ (cm^{-3})	R_{240}	T (K)	$10^{14} k_{10}$[c] ($cm^3\ s^{-1}$)	$10^{15} k_{10}$[d] ($cm^3\ s^{-1}$)	10^{-8}[H][b] ($cm^3\ s^{-1}$)	10^{-8}[OH][b] (cm^{-3})	$10^{-8}[HO_2]$[b] (cm^{-3})	F_{12}	F_{01}
55	14	2.3	11	2.4	0.14	265	4.36	1.46	1.1	1.1	6.0	0.04	4.15
50	12	7.0	8.0	4.5	0.12	270	4.68	1.52	7×10^{-2}	1.0	5.0	0.08	0.68
45	11	15	6.5	8.4	0.11	268	4.55	1.49	7×10^{-4}	0.8	3.0	0.09	0.09
40	8.0	58	3.7	17	0.08	255	3.76	1.33	10^{-5}	0.5	1.0	0.15	0.15

[a] Except where indicated, input data has been taken from ref 4. For the reaction $H + O_3 \rightarrow OH + O_2$, which is necessary to estimate F_{01}, we have used the recommended expression in ref 40 for $220 \leq T/K \leq 360$: $k = 1.4 \times 10^{-10} \exp(-480/T)\ cm^3\ s^{-1}$. [b] Estimated from ref 39. [c] From the recommended expression in ref 40 for $220 \leq T/K \leq 450$, $k = 1.9 \times 10^{-12} \exp(-1000/T)\ cm^3\ s^{-1}$. [d] From the recommended expression in ref 40 for $250 \leq T/K \leq 400$, $k = 1.4 \times 10^{-14} \exp(-600/T)\ cm^3\ s^{-1}$.

vibrationally excited molecules before reaction takes place to form odd oxygen. Naturally, the analysis should entail other factors. For example, the existence of other vibrationally excited species in the upper atmosphere may enhance reactivity through V−V processes (intermolecular transfer), particularly in collisions of O_2 with vibrationally excited N_2: the resulting moderately excited O_2 molecules would then collide with each other to self-deactivate one and self-activate the other. Thus, if the total collisional removal rates k_D and k'_D turn out to be a factor η-fold larger than those assumed in obtaining eq 29, F_{12} (similarly for the other ratios) will be a factor η-fold smaller. For example, if one chooses $\eta = 12.5$ to allow for the fact that only about 8% of the collisions are predicted to involve $OH(v') + O_2(v'')$ in vibrational states that lead to reaction, F_{01} will still be twice the Wodtke ratio at 55 km (and probably significantly larger at higher altitudes). Of course, we have ignored all but a particular[4] vibrational distribution of O_2 (such distributions take place over a continuous range of photodissociation wavelengths), since an exhaustive treatment would be out of scope of the present work. In any case, the assumptions made seem a lot more plausible than to assume thermal equilibration at such high, rarefied, regions of the atmosphere. Thus, the O_x mechanism of Wodtke and co-workers[4] or our revision of it[5,6] together with the novel HO_x cycles may offer an important clue to the "ozone deficit" problem in the upper stratosphere and lower mesosphere where hydrogen−oxygen systems are by far the most reactive ones.

Finally, we examine briefly the implications of the above HO_x mechanisms on the HO_2 concentration at the upper stratosphere and lower mesosphere. Because standard HO_x chemistry is known to overestimate the OH abundance below ~75 km, Summers et al.[41] suggested a reduction by 50%−70% on the rate of $O + HO_2$ reaction to resolve such a hydroxyl surplus. Although it helps to explain also the "ozone deficit" problem, such a downscaling conflicts with available theoretical results[6,47] and the recommended data.[40] Moreover, it leads to large underestimates of the observed abundances[48] of OH and HO_2. On the other hand, the rate constants for reactions 21−23 are larger than for reactions 12−14, which suggests that the hydroxyl radicals are removed at a faster rate than hydroperoxyl ones. The new HO_x mechanisms can therefore provide an explanation for the "ozone deficit" problem (while complementing the reformulated O_x cycle[4,5] at the lower altitudes) and simultaneously help to explain the "OH surplus" in the lower mesosphere, an issue that we hope to revisit elsewhere[49] in relation to the so-called "HO_x dilemma".[42] Needless to say, the consideration of such mechanisms by no means discards that some downscaling[41] of the rate of $O + HO_2$ reaction within its error limits may still be useful.[5]

4. Concluding Remarks

To the extent that the final distributions from the trajectory simulation studies carried out in the present work may represent the actual collisional processes in the high atmosphere, the above findings support our claim that vibrationally hot O_2 is formed there copiously and not rapidly quenched. Despite a somewhat higher degree of vibrational quenching due mainly to the low rotational energies involved, similar conclusions can possibly be extracted for the vibrationally hot hydroxyl radical formed from reaction 6. Thus, there are reasons to believe that the populations of vibrationally excited O_2 and OH will roughly be maintained on an average sense under the environment of the high atmosphere. Although similar studies would be useful for the $O_2(v) + N_2$ and $OH(v) + N_2$ processes, we see no reason of principle for expecting a different result since N_2 is known to be a poorer quencher of both $O_2(v)$ and $OH(v)$ than O_2.

We have also reformulated the HO_x cycle for ozone depletion to become a source of stratospheric O_3. Although much work on such a cycle has been done by other groups, we believe that the focus on the atmospheric implications of HO_x reactions with vibrationally excited O_2 is unique thus far. Clearly, it is too early to assess the impact of the present proposition. While upgrading the theory may not change the major trends concerning the elementary reactions, *LTD atmospheric modeling* would definitely be valuable to resolve some standing issues addressed in the present work.

Acknowledgment. I thank P. J. S. B. Caridade and L. Zhang for computational assistance. Stimulating discussions with Professor H. Teitelbaum (University of Ottawa) and helpful correspondence with Dr. P. C. Cosby (SRI International) are also greatly appreciated. This work has the support of Fundação para a Ciência e a Tecnologia, Portugal.

References and Notes

(1) Chapman, S. *Mem. R. Metereol. Soc.* **1930**, *III*, 103.
(2) Slanger, T. G.; Jusinski, L. E.; Black, G.; Gadd, G. E. *Science* **1988**, *241*, 945.
(3) Slanger, T. G. *Science* **1994**, *265*, 1817.
(4) Miller, R. L.; Suits, A. G.; Houston, P. L.; Toumi, R.; Mack, J. A.; Wodtke, A. M. *Science* **1994**, *265*, 1831.
(5) Varandas, A. J. C. *ChemPhysChem* **2002**, *3*, 433.
(6) Varandas, A. J. C. *Int. Rev. Phys. Chem.* **2000**, *19*, 199.
(7) Geiser, J.; Dylewski, S. M.; Mueller, J. A.; Wilson, R. J.; Toumi, R.; Houston, P. L. *J. Chem. Phys.* **2000**, *112*, 1279.
(8) Daniels, M. J.; Wiesenfeld, J. R. *J. Chem. Phys.* **1993**, *98*, 321.
(9) Varandas, A. J. C.; Pais, A. A. C. C. *Theoretical and Computational Models for Organic Chemistry*; Formosinho, S., Czismadia, I., Arnaut, L., Eds.; Kluwer: Dordrecht, 1991; p 55.
(10) Mack, J. A.; Huang, Y.; Wodtke, A. M.; Schatz, G. C. *J. Chem. Phys.* **1996**, *105*, 7495.
(11) Varandas, A. J. C.; Llanio-Trujillo, J. L. *J. Theor. Comput. Chem.* **2002**, *1*, 31.
(12) Hickson, K. M.; Sharkey, P.; Smith, I. W. M.; Symonds, A. C.; Tuckett, R. P.; Ward, G. N. *Phys. Chem. Chem. Phys.* **1998**, *94*, 533.
(13) Coletti, C.; Billing, G. D. *Chem. Phys. Lett.* **2002**, *356*, 14.
(14) Finlayson-Pitts, B. J.; Pitts, J. N., Jr. *Atmospheric Chemistry;* Wiley: New York, 1986.
(15) Pendleton, W. R., Jr.; Epsy, P. J.; Hammond, M. R. *J. Geophys. Res.* **1993**, *98*, 11567.

(16) Dodd, J. A.; Lipson, S. J.; Lowell, J. R.; Armstrong, P. S.; Blumberg, W. A. M.; Nadile, R. M.; Adler-Golden, S. M.; Marinelli, W. J.; Holtzclaw, K. W.; Green, B. D. *J. Geophys. Res.* **1994**, *99*, 3559.
(17) Meinel, A. B. *Astrophys. J.* **1950**, *111*, 555.
(18) Ohoyama, H.; Kasai, T.; Yoshimura, Y.; Kuwata, H. *Chem. Phys. Lett.* **1985**, *118*, 263.
(19) Dodd, J. A.; Lipson, S. J.; Blumberg, W. A. M. *J. Chem. Phys.* **1991**, *95*, 5752.
(20) Shalashilin, D. V.; Michtchenko, A. V.; Umanskii, S.; Gershenzon, Y. M. *J. Phys. Chem.* **1995**, *99*, 11627.
(21) Knutsen, K.; Dyer, M. J.; Copeland, R. A. *J. Chem. Phys.* **1996**, *104*, 5798.
(22) Varandas, A. J. C.; Zhang, L. *Chem. Phys. Lett.* **2001**, *340*, 62.
(23) Garrido, J. D.; Caridade, P. J. S. B.; Varandas, A. J. C. *J. Phys. Chem. A* **2002**, *106*, 5314.
(24) Hase, W. L.; Duchovic, R. J.; Hu, X.; Komornicki, A.; Lim, K. F.; Lu, D.; Peslherbe, G. H.; Swamy, K. N.; Linde, S. R. V.; Varandas, A. J. C.; Wang, H.; Wolf, R. J. *QCPE Bull.* **1996**, *16*, 43.
(25) Varandas, A. J. C.; Brandão, J.; Pastrana, M. R. *J. Chem. Phys.* **1992**, *96*, 5137.
(26) Caridade, P. J. S. B.; Sabin, J.; Garrido, J. D.; Varandas, A. J. C. *Phys. Chem. Chem. Phys.* **2002**, *4*, 4959.
(27) Caridade, P. J. S. B.; Zhang, L.; Garrido, J. D.; Varandas, A. J. C. *J. Phys. Chem. A* **2001**, *105*, 4395.
(28) Caridade, P. J. S. B.; Betancourt, M.; Garrido, J. D.; Varandas, A. J. C. *J. Phys. Chem. A* **2001**, *105*, 7435.
(29) Varandas, A. J. C.; Yu, H. G. *Mol. Phys.* **1997**, *91*, 301.
(30) Cosby, P. C. July 2002. Private communication.
(31) Osterbrock, D. E.; Fulbright, J. P.; Cosby, P.; Barlow, T. A. *Publ. Astron. Soc. Pac.* **1998**, *110*, 1499.
(32) Polanyi, J. C.; Sloan, J. J. *Int. J. Chem. Kinet. Symp.* **1975**, *1*, 51.
(33) Charters, P. E.; Macdonald, R. G.; Polanyi, J. C. *Appl. Opt.* **1971**, *10*, 1747.
(34) Llewellyn, J.; Long, B. H. *Can. J. Phys.* **1978**, *56*, 581.
(35) Kliner, A. V.; Farrow, R. L. *J. Chem. Phys.* **1999**, *110*, 412.
(36) Dodd, J. A.; Lockwood, R. B.; Hwang, E. S.; Miller, S. M.; Lipson, S. J. *J. Phys. Chem. A* **1999**, *103*, 7834.
(37) Yu, H. G.; Varandas, A. J. C. *J. Chem. Soc., Faraday Trans.* **1997**, *93*, 2651.
(38) Chalamala, B. R.; Copeland, R. A. *J. Chem. Phys.* **1993**, *99*, 5807.
(39) Steinfeld, J. I.; Francisco, J. S.; Hase, W. L. *Chemical Kinetics and Dynamics*; Prentice Hall: Englewood Cliffs, New Jersey, 1989.
(40) Atkinson, R.; Baulch, D. L.; Cox, R. A.; Hampson, Jr., R. F.; Kerr, J. A.; Rossi, M. J.; Troe, J. *J. Phys. Chem. Ref. Data* **1997**, *26*, 521.
(41) Summers, M. E.; Conway, R. R.; Siskind, D. E.; Stevens, M. H.; Offermann, D.; Riese, M.; Preusse, P.; Strobel, D. F.; Russell, J. M., III *Science* **1997**, *277*, 1967.
(42) Conway, R. R.; Summers, M. E.; Stevens, M. H.; Cardon, J. G.; Preusse, P.; Offermann, D. *Geophys. Res. Lett.* **2000**, *27*, 2613.
(43) Zhang, L.; Varandas, A. J. C. *Phys. Chem. Chem. Phys.* **2001**, *3*, 1439.
(44) Varandas, A. J. C.; Caridade, P. J. S. B. *Chem. Phys. Lett.* **2001**, *339*, 1.
(45) Zhang, L.; Varandas, A. J. C. *J. Phys. Chem. A* **2001**, *105*, 10347.
(46) Varandas, A. J. C.; Zhang, L. *J. Phys. Chem. A* **2002**, *106*, 11911.
(47) Setokuchi, O.; Sato, M.; Matuzawa, S. *J. Phys. Chem. A* **2000**, *104*, 3204.
(48) Osterman, G. B.; Salawitch, R. J.; Sen, B.; Toon, G. C.; Stachnik, R. A.; Pickett, H. M.; Margitan, J. J.; Blavier, J.; Peterson, D. B. *Geophys. Res. Lett.* **1997**, *24*, 1107.
(49) Varandas, A. J. C. To be submitted for publication.